Inducible volatile chemical signalling drives antifungal activity of *Trichoderma hamatum* GD12 during confrontation with the pathogen *Sclerotinia sclerotiorum*

Gareth A. Thomas[1,2*], József Vuts[1], David M. Withall[1], John C. Caulfield[1], John Sidda[3], Murray R. Grant[3], Christopher R. Thornton[2], Michael A. Birkett[1]

1. Protecting Crops and the Environment, Rothamsted Research, Harpenden, AL5 2JQ
2. Biosciences, College of Life and Environmental Sciences, University of Exeter, Exeter, EX4 4QD
3. School of Life Sciences, University of Warwick, Coventry, CV4 7AL

*Corresponding author

Abstract

BACKGROUND: The use of beneficial soil fungi or their natural products offers a more sustainable alternative to synthetic fungicides for pathogen management in crops. Volatile organic compounds (VOCs) produced by such fungi act as semiochemicals that inhibit pathogens, with VOC production influenced by physical interactions between competing fungi. This study explores the interaction between the beneficial soil fungus *Trichoderma hamatum* GD12 strain (GD12), previously shown to antagonize crop pathogens such as *Sclerotinia sclerotiorum*, to test the hypothesis that its antagonistic effect is mediated by volatile chemical signalling. A GD12 mutant deficient in the chitinolytic enzyme *N*-acetyl-β-glucosaminidase (*ΔThnag::hph*), which shows reduced biocontrol activity, was also examined**.**

RESULTS: In dual-culture confrontation assays, co-inoculation of GD12 and *S. sclerotiorum* led to fungistatic interactions after 7 days, whereas *ΔThnag::hph* showed no antagonism, indicating a loss of antagonistic function. VOCs collected from individual and co-cultures were analysed by gas chromatography – flame ionization detector (GC-FID) analysis and coupled GC-mass spectrometry (GC-MS), revealing significant differences in VOC production between treatments, with VOC production notably upregulated in the GD12 + *S. sclerotiorum* co-culture. Peak production of 6-pentyl-2H-pyran-2-one occurred 17 days post-inoculation. This upregulation was absent in the *ΔThnag::hph* co-culture, suggesting VOCs may drive antagonism. Synthetic VOC assays revealed several compounds inhibitory to *S. sclerotiorum*, including 1-octen-3-one, which also arrested the growth of key fungal

pathogens (*Botrytis cinerea*, *Pyrenopeziza brassicae*, and *Gaeumannomyces tritici*). Structural insights into 1-octen-3-one's antifungal activity against *S. sclerotiorum* are also presented.

CONCLUSIONS: These findings support the hypothesis that the antagonistic properties of *T. hamatum* GD12 against crop fungal pathogens can, in part, be attributed to VOC production. Further research is needed to assess the potential of these semiochemicals as tools for pathogen management in agriculture.

Keywords: *Trichoderma*, *Sclerotinia sclerotiorum*, volatile organic compounds, antagonism, 1-octen-3-one

Introduction

Sclerotinia sclerotiorum (Lib.) de Bary (Family: Sclerotiniaceae) is a ubiquitous soil-borne fungal pathogen, affecting approximately 800 plant species worldwide, including economically important agricultural crops such as carrots, lettuce, sunflower, oilseed rape and potato (Boland *et al.*, 1994; Bolton *et al.*, 2006a). Management of *S. sclerotiorum* on agricultural crops relies mainly on the application of synthetic fungicides (Derbyshire and Denton-Giles, 2016), although the over-application of fungicides has increased selective pressure, leading to an increase in frequency of fungicide-resistant strains (Ma *et al.*, 2009). Alternative methods for controlling *S. sclerotiorum* include the use of crop rotations, which may also be ineffective due to the formation of vegetative sclerotia by *S. sclerotiorum,* which can remain viable in the soil for over eight years and are resistant to physical, chemical and biological degradation (Tribe, 1957; Adams, 1979; Bolton *et al.*, 2006a). Moreover, engineering crop resistance towards the pathogen has also proven challenging due to differing pathovars of the pathogen, and a lack of resistance in major crops, making breeding programmes a challenge (Bolton et al., 2006; Derbyshire et al., 2022). Therefore, more sustainable approaches for pathogen management on crops, that minimise reliance on synthetic fungicides, are needed.

Sustainable management strategies for the control of *S. sclerotiorum* include the exploitation of microbial biocontrol agents of the pathogen, including beneficial soil fungi. These decrease the negative potential of pathogens on crops through direct antagonism of the pathogen, competition for resources (e.g. nutrients), or through modification of plant defence responses (Ghorbanpour *et al.*, 2018). *Trichoderma* (Hypocreaceae) is a well-studied genus of beneficial soil fungi due to their ability to inhibit fungal pathogen development, induce plant defence responses against pathogens and promote plant growth (Druzhinina *et al.*, 2011; Woo *et al.*, 2023). GD12, a strain of *T. hamatum*, is effective at suppressing the growth of *S. sclerotiorum* in peat-based microcosms (Ryder *et al.*, 2012 Studholme *et al.*, 2013; Shaw *et al.*, 2016), with the suppressing capability of GD12 requiring the chitinase gene *N*-acetyl-β-glucosaminidase (Ryder et al., 2012). Genome sequencing of *Trichoderma hamatum* (Feng *et al.*, 2025) and specifically GD12 (Studholme et al., 2013) reveals the presence of silent gene clusters which could be activated in the presence of antagonistic microorganisms in soil, leading to the production of secondary metabolites which are not produced under standard laboratory conditions (Shaw et al., 2016). This antagonism can stimulate the induction of secondary metabolite biosynthetic gene clusters as evidenced by induction of genes encoding predicted polyketide synthases (PKSs) and Non-Ribosomal Peptide Synthetases (NRPSs) clusters during the interaction between *S. sclerotiorum* and *T. hamatum* in peat microcosms (Shaw *et al.*, 2016). However, the causal metabolites involved in these interactions are currently unknown.

72 Volatile organic compounds (VOCs) are a class of low molecular weight secondary metabolites
73 produced by soil microorganisms, which contribute to their ability to compete against neighbouring
74 organisms for resources in soil (Garbeva and Weisskopf, 2020; Weisskopf *et al.*, 2021). The ability of
75 VOCs to travel between gas- and water-filled pockets in soil classifies them as long-distance
76 messengers, compared to non-volatile secondary metabolites, which may be drivers of more local
77 interactions (Kai *et al.*, 2016; Schulz-Bohm *et al.*, 2017; Westhoff *et al.*, 2017). Microbial VOCs are
78 involved in a range of biological activities, including direct inhibition of pathogenic microorganisms
79 (Fernando *et al.*, 2005), induced plant defence against pathogens (Ryu *et al.*, 2004) and plant growth
80 promotion (Ryu *et al.*, 2003). Several studies indicate *Trichoderma* VOCs can specifically play an
81 inhibitory role against a range of fungal pathogens (Amin *et al.*, 2010; Stoppacher *et al.*, 2010; Jeleń
82 *et al.*, 2014a; Meena *et al.*, 2017; Wonglom *et al.*, 2020). These biological activities highlight the
83 potential for microbial VOCs to be used as effective alternatives to pesticides and fertilisers (Thomas
84 *et al.*, 2020, 2023).

85 Whilst beneficial soil microbes can produce VOCs when grown axenically under standard
86 laboratory conditions, they exist in complex communities within the soil matrix. Genome sequencing
87 of fungal species indicates that many secondary metabolite gene clusters are silent and telomeric
88 under standard laboratory conditions and may require specific cultivation conditions to activate them,
89 including stress inducing, or co-culturing with different species of microorganisms (Scherlach and
90 Hertweck, 2021). Experimentally reproducing a more natural microbe interaction environment is
91 feasible through inoculating different species of microorganisms within the same confined space. Such
92 an approach may stimulate the antagonism that activate silents gene clusters, and hence facilitate the
93 discovery of novel, bioactive compounds. It has been observed that ornesillic acid production was
94 uniquely induced through co-culturing of *Streptomyces* and *Aspergillus* (Schroeckh *et al.*, 2009). This
95 study subsequently led to an expansion in the discovery of novel secondary metabolite production
96 through microbial co-culture (Knowles *et al.*, 2022). For example, in *T. harzianum,* co-culture with the
97 endophyte *Talaromyces pinophilus* led to changes in secondary metabolite production relative to
98 monoculture controls (Vinale *et al.*, 2017). The majority of these studies focus on changes in non-
99 volatile compound production during physical interactions, however a growing body of evidence
100 suggests co-culturing can also induce VOC production, with examples from fungal-fungal (Hynes *et al.*,
101 2007a; Evans *et al.*, 2008; El Ariebi *et al.*, 2016; Guo *et al.*, 2019a; O'Leary *et al.*, 2019), bacterial-
102 bacterial (Tyc *et al.*, 2015, 2017) or fungal-bacterial (Albarracín Orio *et al.*, 2020) interactions.

103 Here, we aimed to determine the role of VOCs in the biocontrol capabilities of *T. hamatum*
104 GD12 against *S. sclerotiorum*. We demonstrate; i) quantitative and qualitative changes in VOC
105 production by *T. hamatum* occur during confrontation with *S. sclerotiorum*; ii) temporal changes in

106 VOC production during confrontation occur, with maximal induction day 17 post inoculation; iii) VOCs
107 produced by *T. hamatum* have antifungal activity against *S. sclerotiorum*; iv) identification of 1-octen-
108 3-one, which completely inhibits the growth of *S. sclerotiorum* as well as other agriculturally important
109 fungal pathogens; and iv) the structural features required for the antifungal activity of 1-octen-3-one
110 against *S. sclerotiorum*. This work highlights the power of using *Trichoderma*-pathogen co-culture to
111 reveal cryptic chemistries encoding bioactive VOCs for use as pathogen management tools in
112 agriculture.

113

114 **Materials and methods**

115 *Dual-culture confrontation assays. Trichoderma hamatum* GD12 isolated from a potato field (Great
116 Down, Devon, UK), (Thornton, pers. comm.), *ΔThnag : : hph* : : *hph* (Ryder et al., 2012) and *Sclerotinia*
117 *sclerotiorum* isolate 1 (isolated on oilseed rape petal, ADAS Rosemaund, Herefordshire, UK), (West,
118 pers. comm.), used in the study were maintained on Potato Dextrose Agar (PDA) (15 g Bacteriological
119 Agar No. 2, LabM, UK; 24 g Potato Dextrose Broth (PDB), Sigma, UK; 1000 mL distilled H_2O) slopes in
120 sterile, screw-capped plastic vials (ThermoScientific, UK). Circular plugs (5 mm diam.) were cut using
121 a sterilised cork-borer (Sigma, UK) from the leading edge of mycelia of 3-day old PDA plates of *T.*
122 *hamatum* (GD12, *ΔThnag : : hph*) or *S. sclerotiorum* isolate 1. Each experiment comprised (a) a control,
123 containing uninoculated growth media (PDA), (b) the confrontation of a *T. hamatum* strain co-cultured
124 against itself (self-challenged), (c) the *S. sclerotiorum* co-cultured against itself (self-challenged), and
125 (d) the *T. hamatum* strain challenged against *S. sclerotiorum* (co-culture) (n=4). Plugs from individual
126 strains of *T. hamatum* were placed approximately 80 mm away from plugs of *S. sclerotiorum* on fresh
127 PDA plates (90 mm) and grown for 7 days under a 16 h/8 h fluorescent light/dark photoperiod at 24°C
128 until required for dynamic headspace collection experiments (detailed below).

129 *Dynamic headspace collection (air entrainment).* PDA plates containing 7-day-old fungal cultures (see
130 above) were enclosed individually in glass entrainment vessels (12 cm diam. x 6 cm height). Charcoal-
131 purified air (flowrate 600 mL/min) was pushed into each entrainment vessel and drawn (flowrate 500
132 mL/min), ensuring a positive pressure (100 mL/min) throughout the system. Air was drawn through a
133 glass tube containing Porapak Q (50 mg, 50/80 mesh, Supelco, Bellefonte, PA) held with two plugs of
134 silanized glass wool, for 20 h at ambient temperature (Pye volatile collection kits, Kings Walden, UK).
135 Before each collection, glass vessels were washed with Teepol detergent, rinsed with distilled water,
136 washed with acetone (ThermoFisher, UK), and then placed in a modified heating oven (180°C) for a
137 minimum of 2 h. Charcoal filters (10-14 mesh, 50 g) (Sigma, UK) were conditioned prior to each
138 experiment by attaching them to a supply of nitrogen in a modified heating oven (150°C) under a

139 constant stream of nitrogen. Volatile collections were performed under a 16 h/8 h light/dark
140 photoperiod at 24°C. Porapak Q traps were cleaned by washing with freshly redistilled diethyl ether
141 (2 mL) and heated to 132°C for a minimum of 2 h under a stream of nitrogen. Following collections,
142 VOCs were eluted from the Porapak Q traps with freshly redistilled diethyl ether (750 µL) into 1.1 mL
143 pointed vials (ThermoScientific, Germany), capped with an 8 mm Chromacol screw cap vial lid
144 (ThermoScientific, Germany) with an 8 mm Silicone Red PTFE Septa (Kinesis, UK). The eluent was
145 concentrated to 50 µL under a gentle stream of nitrogen and stored at -20°C prior to further analysis.

146 *Time-course VOC collection experiment.* Solid-phase microextraction (SPME) was selected as the
147 method for VOC analysis for time-course experiments rather than dynamic headspace collection, as
148 preliminary experiments showed repeated dynamic headspace collections of VOCs from fungal
149 cultures led to drying out of growth media, impacting fungal growth. An SPME (100 µM
150 Polydimethylsiloxane (PDMS) fibre, Supelco, UK) was introduced into the GC thermal desorption
151 injector port to desorb for 10 min (temperature of injector=250°C). The SPME fibre was inserted
152 through a clean septum and exposed to the headspace of the fungal culture within a clean glass
153 entrainment vessel (12 cm diam. x 6 cm height) for 1 h. SPME samples were taken at 1, 2, 3, 4, 5, 6 ,7,
154 10, 17 and 24 days post inoculation (dpi) from cultures of (a) self-challenged *S. sclerotiorum* isolate 1,
155 (b) self-challenged *T. hamatum* GD12, or (c) GD12 co-cultured with *S. sclerotiorum*. The first sampling
156 timepoint (day 1 post inoculation) of the experiment was used as a baseline, with 80 mm of distance
157 between the fungal mycelia. At day 2, the distance between the self-challenged GD12 treatments was
158 19-24 mm, and 7-15 mm for the GD12 co-cultured with *S. sclerotiorum* treatments. Self-challenged *S.*
159 *sclerotiorum* treatments had already initiated contact by this stage of sampling. By day 3, contact
160 between mycelia across all treatments had established.

161 *Gas chromatography – flame ionization detector (GC-FID) analysis.* Air entrainment samples were
162 analysed on an Agilent 6890 GC equipped with a cool on-column injector, an FID and a HP-1 bonded-
163 phase fused silica capillary column (50 m x 0.32 mm i. d. x 0.52 µm film thickness). The oven
164 temperature was set at 30°C for 0.1 min, then increased at 5°C/min to 150°C for 0.1 min, then at
165 10°C/min to 230°C for a further 25 min. The carrier gas was hydrogen. VOCs adsorbed on SPME fibres
166 were thermally desorbed by inserting the fibre directly into the OPTIC Programmable Temperature
167 Vaporisor (PTV) unit (30 -> 250℃ ballistically at a rate of 16℃/s).

168 *Coupled GC-mass spectrometry (GC-MS).* An Agilent Mass Selective Detector (MSD) 5973 coupled to
169 an Agilent 6890N GC (fitted with a non-polar HP1 column 50 m length x 0.32 mm i. d. x 0.52 µM film
170 thickness, J & W Scientific) was used for analysis. Sample injection was via cool-on column and MS
171 ionization was by electron impact at 70 eV at 220°C. The GC oven temperature was maintained at 30°C

172 for 5 min and then programmed at 5°C/min to 250°C, run time 70 minutes. Tentative identifications
173 were confirmed by co-injections with authentic standards (Pickett et al., 1990).

174 *Chemicals.* 1-Pentanol (99%), 1-octen-3-ol (98%), 1-octene (98%), 2-undecanone (99%), 2-octanone
175 (98%), 3-octanone (99%), 2-pentylfuran (≥ 98%), 6-*n*-pentyl-2H-pyran-2-one (6-PAP) (≥ 96%), 1-octen-
176 3-one (96%) and 2-heptanone (98%) were all purchased from Sigma-Aldrich, UK. Diethyl ether (99.5%)
177 was purchased from Fisher and redistilled before use.

178 *Synthetic compound assays.* Synthetic standards of VOCs identified from air entrainments of *T.*
179 *hamatum* GD12 were applied to sterile qualitative filter paper (6 mm) (Whatman, UK) and placed onto
180 a Petri dish containing PDA. On a fresh plate of PDA, a plug (5 mm diam.) of *S. sclerotiorum* was
181 inoculated and the plate inverted over another plate containing the filter paper with the synthetic
182 VOC sample, and the two plates were then sealed with tape, ensuring no physical contact between
183 the VOC sample and the pathogen (Figure S1). Solutions of VOCs were prepared in freshly redistilled
184 diethyl ether to ensure that 20 µL application of solution gave a dose of 45.5 µM. This dose was
185 decided based on preliminary experiments, where 5 µL of each compound were applied neat to a
186 sterile filter paper, and the dose selected based on the least inhibitory compound (1-pentanol; 5 µL of
187 which equates to 45.5 µM). This dose is similar to that used in previous studies (Tyc *et al.*, 2015). For
188 compounds demonstrating significant ($p < 0.05$) antifungal activity relative to control treatments
189 when applied at 45.5 µM, doses onto filter discs were diluted to 22.75 µM, 11.125 µM, 4.55 µM, 2.275
190 µM, 0.91 µM and 0.455 µM in freshly redistilled diethyl ether from a stock solution, until no further
191 inhibition was observed. Mycelial measurements from *S. sclerotiorum* were taken using a 30 cm ruler
192 after 72 h. From the diameter of *S. sclerotiorum*, the area of colony was calculated as πr^2, where "r" is
193 equal to the radius of the colony. Control plates contained a sterile filter paper disc with 20 µL of
194 freshly redistilled diethyl ether alone.

195 *Statistical analysis.* For comparison of GC analysis from confrontation assays, peak area values were
196 individually measured (Agilent Chemstation) and $\log_{10}$-transformed. An adjustment of 0.001 was
197 applied to account for values recorded as zero. Statistical comparison of compounds present in both
198 mono- and co-culture treatments were analysed using an unpaired Student's t-test assuming equal
199 variances, one variate with grouped factor. To establish the antifungal activity of selected VOCs,
200 mycelial areas were statistically compared across treatments using one way analysis of variance
201 (ANOVA), followed by Tukey's Honest Significant Difference test at the $p < 0.05$ level, where multiple
202 comparisons were required. Genstat® (v21, ©VSN International, Hemel Hempstead, UK) was used for
203 all statistical analyses.

204

205 **Results**

206 Dual-culture confrontation assays demonstrated fungistatic interactions between *T.*
207 *hamatum* GD12 when confronted with *S. sclerotiorum* after 7 days of growth (Figure 1). This was
208 accompanied by the formation of yellow spores by *T. hamatum* GD12 in the interaction zone between
209 the two fungi. Contrastingly, during confrontation with *T. hamatum ΔThnag::hph*, overgrowth of *S.*
210 *sclerotiorum* was observed, depicted by a black arrow (Figure 1f), indicating a loss in the antagonistic
211 capabilities of the *ΔThnag::hph* mutant.

212 Significant quantitative and qualitative changes in VOC production compared to self-
213 challenged GD12 treatments were observed when *T. hamatum* GD12 was co-cultured with *S.*
214 *sclerotiorum* (Figure 2; Table 1). Production of 6-pentyl-2H-pyran-2-one (6-PAP) dominated the
215 headspace of GD12 co-cultured with *S. sclerotiorum*, with mean production of 6-PAP significantly
216 greater in these co-cultures compared to self-challenged controls ($p < 0.001$) (Table 1). Of the 36
217 compounds detected, eight of which were confirmed by co-injection, 22 were unique to GD12-*S.*
218 *sclerotiorum* co-cultures, suggesting that the VOCs were either biosynthesised *de novo* in the presence
219 of *S. sclerotiorum* or produced below detectable limits of the GC in GD12 monocultures, including 2-
220 pentylfuran (Figure 2; Table 1).

221 As co-culturing *T. hamatum* GD12 with *S. sclerotiorum* led to significant increases in VOC
222 production, the temporal dynamics of *T. hamatum* GD12 VOC production was investigated. For three
223 compounds detected by SPME, peak induction was greatest at day 17 post-co-culture, each
224 subsequently by day 24 (Figure 3). Each compound showed similar trends in production across the
225 different timepoints. In GD12 co-cultured with *S. sclerotiorum* treatments, compound 1 (KI = 1252)
226 was not detected in the headspace until day 6. By day 10 there was an increase in production, which
227 further increased at day 17, subsequently decreasing to day 24. 6-PAP shows a similar trend.
228 Compound 2 (KI = 1994), detected by day 10, increasing until day 17, and then decreasing by day 24.

229 When co-cultured with *S. sclerotiorum*, quantitative and qualitative changes in VOC
230 production relative to self-challenged *ΔThnag::hph* treatments were observed, although unlike with
231 GD12, most VOCs were either down-regulated during co-cultivation, or not significantly different to
232 self-challenged controls (Figure 4). This provides a negative control to directly link unique GD12 VOC
233 production to biocontrol. Four of the 10 VOCs detected are up-regulated in self-challenged
234 *ΔThnag::hph* treatments relative to *ΔThnag::hph* co-cultured with *S. sclerotiorum*, and five were not
235 significantly different to controls (Table 2). Notably, 6-PAP, showing the greatest induction in GD12
236 co-cultured with *S. sclerotiorum* treatments, was present in *ΔThnag::hph* monocultures, but not in
237 three out of four replicates in *ΔThnag::hph* co-cultured *S. sclerotiorum* treatments. Four VOCs (KI =

238 1552; KI = 2016; KI =2055; KI = 2264) were significantly greater in self-challenged *ΔThnag : : hph* relative
239 to co-culture treatments, and five were not significantly different. Taken together, these findings
240 indicate a direct or indirect role for the *N*-acetyl-β-glucosaminidase enzyme in the induction of VOCs
241 by *T. hamatum* GD12 during confrontation with *S. sclerotiorum*.

242 In preliminary experiments with *T. hamatum* VOCs and *S. sclerotiorum*, 6-PAP had no
243 detectable inhibitory activity against *S. sclerotiorum* ($F_{2,6}$=2.17, p = 0.195) (Figure S2) and was
244 therefore excluded from further bioassays. The mycelial area of *S. sclerotiorum* differed significantly
245 depending on the specific VOC applied at the highest dose (45.5 µM), indicative of differences in their
246 inhibitory activities ($F_{7,16}$= 171.36; p < 0.001; n= 3) (Figure 5). The mycelial area of *S. sclerotiorum*
247 exposed to 1-pentanol was not significantly different to solvent control treatments (P > 0.05), and 2-
248 heptanone treatments were not significantly different to 1-pentanol treatments (P > 0.05), so these
249 compounds were not tested at reduced doses. 2-octanone and 2-undecanone demonstrated similar
250 levels of inhibition, while 2-octanone was significantly more inhibitory than 3-octanone. Strikingly, 1-
251 octen-3-one demonstrated effectively complete growth of inhibition of *S. sclerotiorum*. Importantly,
252 this antifungal activity was effective against other economically fungal pathogens (*Botrytis cinerea*,
253 *Pyrenopeziza brassicae* and *Gaeumannomyces tritici*) (Figure S3).

254 Of the tested VOCs, the five demonstrating the most significant inhibition were selected for
255 further study at reduced doses, and all demonstrated significant inhibition when applied at reduced
256 doses; 1-octen-3-one: ($F_{7,16}$= 246.03; p < 0.001); 2-octanone: ($F_{3,8}$= 42.29; p < 0.001); 3-octanone:
257 ($F_{4,10}$= 31.74; p < 0.001); 2-pentylfuran: ($F_{5,12}$= 119.2; p < 0.001) and 2-undecanone: ($F_{7,16}$= 91.65; p <
258 0.001) (Figure 5). 2-octanone had a minimum inhibitory dose of 11.125 µM, 3-octanone, 2-pentylfuran
259 had a minimum inhibitory dose of 4.55 µM and 2-undecanone, 2.275 µM (Figure 6). The compound
260 showing the greatest inhibition, 1-octen-3-one, was still significantly inhibitory at a 100-fold dilution
261 (0.445 µM).

262 To establish potential structural moieties required for antifungal activity of 1-octen-3-one
263 against *S. sclerotiorum*, compounds with similar structural features to both 1-octene, 3-octanone and
264 (*RS*)-1-octen-3-ol were tested (Figure S4), revealing significant differences in inhibitory activities ($F_{4,10}$=
265 114.44; p < 0.001) (Figure 7). 1-octene demonstrated no significant inhibition of *S. sclerotiorum*
266 relative to solvent controls (p > 0.05), whereas both 3-octanone and (*RS*)-1-octen-3-ol showed
267 significant inhibition of *S. sclerotiorum* relative to controls (p < 0.05). However, only 1-octen-3-one
268 demonstrated 100% inhibition. When *S. sclerotiorum* was removed from the shared atmosphere with
269 1-octen-3-one, fungal growth of the pathogen was not restored 4 weeks after removing the pathogen

270 from the headspace (Figure 8). This is consistent with 1-octen-3-one having fungicidal activity at the
271 tested dose.

272

273 **Discussion**

274 In this study, we showed induction of VOC production by *T. hamatum* GD12 during co-culture
275 with the fungal pathogen *S. sclerotiorum*. This included VOCs not produced by *T. hamatum* when
276 grown axenically. This VOC induction was not observed during the interaction between *S. sclerotiorum*
277 and the *ΔThnag::hph* mutant, suggesting a role of the *N*-acteyl-β-glucosaminidase enzyme in the
278 direct or indirect facilitation of VOC induction. Whilst several VOCs were also produced in self-
279 challenged GD12 controls, the stimulation of VOC production in co-cultures indicates a *de novo*
280 biosynthesis in the presence of the pathogen, some of which we demonstrate possess an antifungal
281 role against *S. sclerotiorum*.

282 Many studies investigating VOC production from *Trichoderma* species utilise axenic fungal
283 growth, and VOCs are predominantly assigned to alcohols, ketones, alkanes, furans, mono- and-
284 sesquiterpenes (Jeleń *et al.*, 2014a). Several low molecular weight compounds reported here as being
285 produced by *T. hamatum* GD12 have been previously identified from other *Trichoderma* species,
286 including 3-octanone (Nemčovič *et al.*, 2008; Stoppacher *et al.*, 2010; Jeleń *et al.*, 2014a; Estrada-
287 Rivera *et al.*, 2019; Speckbacher *et al.*, 2020; Silva *et al.*, 2021) and 2-octanone (Jeleń *et al.*, 2014b;
288 Estrada-Rivera *et al.*, 2019; Speckbacher *et al.*, 2020). To our knowledge, this is the first report of 1-
289 octen-3-one being produced by *T. hamatum*, although it was identified from *T. virens* (Li *et al.*, 2018),
290 and a range of other fungi (Pennerman *et al.*, 2022). 6-PAP is a characteristic *Trichoderma* VOC
291 (Mendoza-Mendoza *et al.*, 2024), which produces a coconut aroma (Reithner *et al.*, 2007; Stoppacher
292 *et al.*, 2010; Jeleń *et al.*, 2014a; Garnica-Vergara *et al.*, 2016; Estrada-Rivera *et al.*, 2019; Baazeem *et*
293 *al.*, 2021; Silva *et al.*, 2021). When comparing the *T. hamatum* GD12 VOCs identified via co-culture
294 with other studies, only 6-PAP has been previously reported (Jeleń *et al.*, 2014a; Baazeem *et al.*, 2021).
295 However, directly comparing volatile diversity across other studies should be undertaken with caution
296 as such studies employ different volatile sampling techniques, which can introduce biases for certain
297 compounds. For example, while many studies deploy SPME for headspace sampling, the diversity of
298 fungal volatiles recovered depends on the type of fibre used (Stoppacher et al., 2010; Jeleń et al.,
299 2014). Growth conditions of cultures will also likely vary across studies, which can influence volatile
300 production from *Trichoderma*, including age of cultures (Lee *et al.*, 2015), relative humidity and
301 temperature of growth conditions (Polizzi *et al.*, 2011), as well as media composition (Zhang *et al.*,
302 2014; González-Pérez *et al.*, 2018). Intraspecific differences in volatile production have been observed

303 for *T. hamatum*, as well as within other *Trichoderma* species. This likely relates to fungal
304 evolution/adaptation to different geographical regions or ecological niches from which they were
305 isolated (Jeleń et al., 2014; Lee et al., 2016), but also highlights the power of geographical/niche
306 adaptation to drive the evolution of novel antifungals . Taken together, a range of factors can account
307 for variation in VOC production by *Trichoderma*, both inter- and intra-specifically.

308 Co-cultivation with *S. sclerotiorum* revealed significant quantitative and qualitative changes in
309 volatile production compared to the VOCs produced by *T. hamatum* GD12 in self-challenged controls.
310 This induction was greatest 17 dpi, consistent with other studies (Hynes et al., 2007). 2-Pentylfuran,
311 which was biosynthesised *de novo* in response to the interaction with *S. sclerotiorum*, has previously
312 been reported from *T. hamatum* during axenic culture (Jeleń *et al.*, 2014a). Many of the upregulated
313 compounds in our study are of the sesquiterpene-like class, which have previously been observed
314 during physical fungal-fungal interactions (Hynes *et al.*, 2007a; Guo *et al.*, 2019a; Rajani *et al.*, 2021),
315 including *T. hamatum* when challenged with the ectomycorrhizal fungus *Laccaria bicolor* (Guo *et al.*,
316 2019b) and *Trichoderma* in confrontation with *Sclerotium rolfsii* and *Macrophomina phaseolina*
317 (Sridharan *et al.*, 2020). Sesquiterpenes are a well-known class of compounds involved in chemical
318 signalling, and have been isolated across a range of *Trichoderma* species, including *T. hamatum* (Ma
319 *et al.*, 2021), *T. brevicompactum* (Shi *et al.*, 2020), *T. virens* (Shi *et al.*, 2018, 2021; Hu *et al.*, 2019), *T.*
320 *longibrachiatum* (Du *et al.*, 2020; Wang *et al.*, 2022), *T. asperellum* (Ding *et al.*, 2012), and *T.*
321 *citrinoviride* (Liu *et al.*, 2020). Many of these sesquiterpene-like compounds possess antifungal
322 activities against a range of phytopathogenic fungi, bacteria and marine phytoplankton. As well as
323 their antimicrobial roles, microbial sesquiterpenes have a range of other biological activities including
324 signalling, host growth promotion and defence (Avalos *et al.*, 2022). The upregulation of unknown
325 sesquiterpenes during co-culture of *T. hamatum* and *S. sclerotiorum* could indicat a biological role for
326 these compounds, and future work aims to isolate and identify these compounds to determine their
327 role in the antagonistic response against *S. sclerotiorum*, and potential for integrating into biocontrol
328 strategies.

329 6-PAP dominated the VOC profile of *T. hamatum* GD12 co-cultured with *S. sclerotiorum*,
330 relative to self-challenged *T. hamatum* GD12 cultures, corroborating previous work which found
331 significant increases in 6-PAP production when *T. harzianum* was co-inoculated with *R. solani*
332 (Serrano-Carreón *et al.*, 2004; Flores *et al.*, 2019). Whilst significant increases in 6-PAP production by
333 *T. hamatum* GD12 in co-culture were observed, no antifungal activity was observed when 6-PAP was
334 applied in the inverted plate assay setup (Figure S2). However, several studies demonstrate an
335 inhibitory role for 6-PAP against a range of fungal pathogens, including *Fusarium* species (Scarselletti
336 and Faull, 1994; El-Hasan *et al.*, 2008; Jeleń *et al.*, 2014a; Rao *et al.*, 2022), *Botrytis cinerea* (Pezet *et*

337 *al.*, 1999), *Cylindrocarpon destructans* (Jin *et al.*, 2020), and *Rhizoctonia solani* (Scarselletti and Faull,
338 1994), when the compound was in contact with the pathogens. These studies indicate that 6-PAP may
339 require direct contact for effective antifungal activity. As well as 6-PAP upregulation, 2-octanone
340 production was significantly upregulated in co-culture treatments, indicative of *T. hamatum* - *S.*
341 *sclerotiorum* antagonism. 2-octanone upregulation has also been observed during the interaction
342 between the fungal pathogen *Setophoma terrestris* and the beneficial soil bacteria *Bacillus subtilis*
343 (Albarracín Orio *et al.*, 2020), as well as the interaction between *T. atroviride* and *F. oxysporum*
344 (Speckbacher *et al.*, 2021), indicating a broader spectrum role for this compound in antagonistic fungal
345 interactions.

346 Many of the VOCs produced by *T. hamatum* GD12 during self-challenge and in co-cultures
347 with *S. sclerotiorum* show significant antifungal activity against *S. sclerotiorum*. The antifungal role of
348 2-octanone demonstrated here is in agreement with the inhibition of the soil fungal pathogen
349 *Setaphoma terrestris*, which could indicate broad-spectrum inhibitory activity against a range of fungal
350 pathogens (Albarracín Orio *et al.*, 2020). Similarly, 2-heptanone has previously shown significant
351 inhibition against *Curvularia lunata* (Xie *et al.*, 2020) and *Alternaria solani* (Zhang *et al.*, 2020). Here,
352 we report only moderate antifungal activity of 2-heptanone at the highest tested dose relative to
353 other compounds, which may relate to differences in doses tested across the studies, or specificity in
354 the antifungal activity of 2-heptanone against different pathogenic species. Alternatively, it may
355 reflect that anti-fungal role could be derived from 2-octanone via further modifications that many
356 occur in a more complex soil microbiome, as opposed to our two-component experimental system.
357 Specificity of antifungal activity has been observed for 2-undecanone, which has shown an inhibitory
358 role against *Verticillium dahlia*, *F. oxysporum*, *B. cinerea* and *Monilinia* spp., but not *Penicillium* spp.
359 (Calvo *et al.*, 2020) or *Rhizopus stolonifer* (Carter-House *et al.*, 2020). Having identified a range of
360 antifungal compounds, determining the modes of action of the antifungal activities against *S.*
361 *sclerotiorum* is an important next step. Furthermore, whilst the inhibitory properties of several *T.*
362 *hamatum* VOCs have been demonstrated against *S. sclerotiorum*, it is important to establish that
363 compounds at their inhibitory doses do not have phytotoxic effects. Interestingly, 2-pentylfuran,
364 which was upregulated in the presence of *S. sclerotiorum* and showed an antifungal role against the
365 pathogen, has also demonstrable plant growth-promoting capabilities (Zou *et al.*, 2010). Thus , 2-
366 pentylfuran could potentially be a promising candidate to replace synthetic chemical inputs due to its
367 ability to inhibit fungal pathogens without compromising plant growth.

368 To our knowledge, this is the first report demonstrating an antifungal role for 1-octen-3-one
369 against a pathogen. When structurally related compounds (1-octene, 3-octanone, (*R,S*)-1-octen-3-ol)
370 were tested for their antifungal activity at equivalent doses, 3-octanone and (*RS*)-1-octen-3-ol

371 demonstrated significant inhibition of *S. sclerotiorum*, whereas absolutely no growth of *S. sclerotiorum*
372 occurred when exposed to 1-octen-3-one. It is thus possible that fungicidal activity may be enhanced
373 via Michael-type acceptance by the α,β–unsaturated carbonyl structure within the latter compound
374 (Li *et al*., 2019). Several of the strobilurin class of fungicides (fungicides derived from *Strobilurus spp.*,
375 Nofiani *et al.*, 2018) also contain a conjugated ketone and alkene moiety. Findings here are contrary
376 to those reported by Xiong *et al*. (2017), who found significant inhibition of *F. tricinctum* and *F.*
377 *oxysporum* treated with 1-octen-3-ol, but no inhibition when fungi were treated with 1-octen-3-one
378 (Xiong *et al.*, 2017). However, VOCs were administered differently in each experiment, making cross-
379 comparison difficult. VOCs tested by Xiong et al. were supplemented into growth medium and in direct
380 contact with *Fusarium* species, whereas tested VOCs here were physically separated from *S.*
381 *sclerotiorum,* suggesting that the antifungal effect of 1-octen-3-one works at a distance. An important
382 consideration is that, in both studies, (*RS*)-1-octen-3-ol was tested as a racemic mixture, although
383 previous work has shown chirality can impact its antifungal activity (Yin *et al.*, 2019). Whilst 1-octen-
384 3-one shows an inhibitory role against *S. sclerotiorum*, future work should determine the role of the
385 compound on plant growth. For example, 1-octen-3-one exposure significantly inhibits *Arabidopsis*
386 growth and development (Lee *et al.*, 2019), therefore future work should focus on determining which
387 dose of 1-octen-3-one can inhibit *S. sclerotiorum* without compromising plant growth. Moreover, as
388 seen with antimicrobial drugs, a mixture of antifungals may have synergistic activities, yet overall
389 reduced potential phytotoxic effects, enabling the incorporation of 1-octen-3-one into biocontrol
390 strategies. As compounds identified here have *in vitro* antagonism against *S. sclerotiorum*, immediate
391 priorities will be to test these compounds against *S. sclerotiorum*, individually and in combinations,
392 using peat microcosms under glasshouse conditions. These data will inform future open field trials, to
393 examine their biological activities under more agriculturally relevant conditions.

394 *Trichoderma* spp. recognise plant pathogenic fungi when their lytic enzymes, including *N*-acetyl-*β*-D-
395 glucosaminidase, release small diffusible components from fungal cell walls (Druzhinina *et al.*, 2011).
396 These components can then bind G-Protein Coupled Receptors (GPCRs) on the cell surface of
397 *Trichoderma*, activating a downstream signalling cascade leading to the expression of secondary
398 metabolite biosynthesis genes, potentially including genes linked to volatile production. As
399 *ΔThnag::hph* cannot produce the chitinase enzymes required to break down fungal cell walls,
400 theoretically no breakdown products from *S. sclerotiorum* would bind to the GPCRs of *T. hamatum*,
401 preventing elicitation of the downstream signalling cascade and activation of secondary metabolite
402 biosynthesis genes. Significant reduction in 6-PAP production by the *ΔThnag::hph* mutant during co-
403 culture with *S. sclerotiorum* may also suggest a role for *N*-acetyl-*β*-D-glucosaminidase in 6-PAP
404 production, which several studies have previously demonstrated. For example, deletion of the *tga1*

405 gene, encoding the α-subunit of a heterochromatic G-protein 1 from *T. atroviride*, led to both a
406 reduction in *N*-acetyl-*β*-D-glucosaminidase activity in mutant strains and an 8-fold reduction in 6-PAP
407 production, relative to controls (Reithner *et al.*, 2005). Similarly, deletion of the gene encoding
408 mitogen-activated protein kinase (*tmk1*) led to a 1.6-fold increase in production of 6-PAP and the
409 enhancement of *nag1* expression relative to the parent strain (Reithner *et al.*, 2007). The reduction in
410 6-PAP production by *Δthnag::hph* may also explain why the mutant loses its antagonistic activity
411 against *S. sclerotiorum* in peat microcosms (Ryder *et al.*, 2012).

412 In conclusion, this study suggests a role for volatile chemical signalling during the antagonistic
413 response of *T. hamatum* GD12 against *S. sclerotiorum* and shows that certain *Trichoderma*-derived
414 VOCs play an inhibitory role against the pathogen. Specifically, we identify1-octen-3-one as a potential
415 novel antifungal VOC. Further glasshouse and field tests with antifungal compounds identified here
416 are required to determine whether they inhibit pathogens at a larger scale under more agriculturally
417 relevant conditions. Whilst several of these compounds have been identified here, or previously
418 described, many *T. hamatum* compounds upregulated on confrontation with fungal plant pathogens
419 remain to be identified and characterised.

420

421

422 **Author contributions**

423 Conceptualisation: MB, MG, CT. Data curation; GT, JV, JC, MB. Formal analysis; GT, JC, JV, MB, DW.
424 Funding acquisition; MB, CT, MG. Investigation; MB, GT, MG, CT, JV, DW. Methodology; MB, GT, MG,
425 CT, JS. Project administration; MB, MG, CT. Original draft; GT, MB, DW. Reviewing and editing; GT,
426 MB, DW, JV, CT, MG, JS, JC**.**

427

428 **Acknowledgements**

429 Rothamsted Research receives strategic funding from the Biotechnology and Biological Sciences
430 Research Council of the United Kingdom (BBSRC). We acknowledge support from the Growing Health
431 Institute Strategic Programme (BB/X010953/1; BBS/E/RH/230003A). The work formed part of the
432 Rothamsted Smart Crop Protection (SCP) strategic programme (BBS/OS/CP/000001) funded through
433 BBSRC's Industrial Strategy Challenge Fund. GT's PhD studentship was funded by a Biotechnology and
434 Biological Sciences Research Council (BBSRC) Southwest Doctoral Training Programme award (project
435 no. 1622285). The authors would also like to thank Jon West and Kevin King for providing *Sclerotinia*

sclerotiorum and *Botrytis cinerea*, Lisa Humbert for providing *Pyrenopeziza brassicae*, and Javier Palma-Guerrero for providing *Gaeumannomyces tritici*.

References

Adams, P.B. (1979) Ecology of *Sclerotinia* Species . *Phytopathology* **69**: 896.

Albarracín Orio, A.G., Petras, D., Tobares, R.A., Aksenov, A.A., Wang, M., Juncosa, F., et al. (2020) Fungal–bacterial interaction selects for quorum sensing mutants with increased production of natural antifungal compounds. *Commun Biol*.

Amin, F., Razdan, V.K., Mohiddin, F.A., Bhat, K.A., and Sheikh, P.A. (2010) Effect of volatile metabolites of *Trichoderma* species against seven fungal plant pathogens in-vitro. *Journal of Phytology* **2**: 34–37.

Sridharan, A.P. Thankappan, S., G., K., and Uthandi, S. (2020) Comprehensive profiling of the VOCs of *Trichoderma longibrachiatum* EF5 while interacting with *Sclerotium rolfsii* and *Macrophomina phaseolina*. *Microbiol Res*.

El Ariebi, N., Hiscox, J., Scriven, S.A., Müller, C.T., and Boddy, L. (2016) Production and effects of volatile organic compounds during interspecific interactions. *Fungal Ecol* **20**: 144–154.

Avalos, M., Garbeva, P., Vader, L., Van Wezel, G.P., Dickschat, J.S., and Ulanova, D. (2022) Biosynthesis, evolution and ecology of microbial terpenoids. *Nat Prod Rep* **39**: 249–272.

Baazeem, A., Almanea, A., Manikandan, P., Alorabi, M., Vijayaraghavan, P., and Abdel-Hadi, A. (2021) In Vitro Antibacterial, Antifungal, Nematocidal and Growth Promoting Activities of *Trichoderma hamatum* FB10 and Its Secondary Metabolites. *Journal of Fungi 2021, Vol 7, Page 331* **7**: 331.

Boland, G.J., Hall, & R., and Hall, R. (1994) Index of plant hosts of *Sclerotinia sclerotiorum*. *CANADIAN JOURNAL OF PLANT PATHOLOGY*.

Bolton, M.D., Thomma, B.P.H.J., and Nelson, B.D. (2006a) Sclerotinia sclerotiorum (Lib.) de Bary: Biology and molecular traits of a cosmopolitan pathogen. *Mol Plant Pathol*.

Calvo, H., Mendiara, I., Arias, E., Gracia, A.P., Blanco, D., and Venturini, M.E. (2020) Antifungal activity of the volatile organic compounds produced by *Bacillus velezensis* strains against postharvest fungal pathogens. *Postharvest Biol Technol*.

Carter-House, D., Chung, J., McDonald, S., Mauck, K., and Stajich, J.E. (2020) Volatiles from *Serratia marcescens*, *S. proteamaculans*, and *Bacillus subtilis* Inhibit Growth of *Rhizopus stolonifer* and Other Fungi. *bioRxiv*.

Derbyshire, M.C. and Denton-Giles, M. (2016) The control of sclerotinia stem rot on oilseed rape (*Brassica napus*): current practices and future opportunities. *Plant Pathol* **65**: 859–877.

Derbyshire, M.C., Newman, T.E., Khentry, Y., and Owolabi Taiwo, A. (2022) The evolutionary and molecular features of the broad-host-range plant pathogen *Sclerotinia sclerotiorum*. *Mol Plant Pathol* **23**:.

472 Ding, G., Chen, A.J., Lan, J., Zhang, H., Chen, X., Liu, X., and Zou, Z. (2012) Sesquiterpenes and
473 Cyclopeptides from the Endophytic Fungus *Trichoderma asperellum* Samuels, Lieckf. &
474 Nirenberg. *Chem Biodivers* **9**: 1205–1212.

475 Druzhinina, I.S., Seidl-Seiboth, V., Herrera-Estrella, A., Horwitz, B.A., Kenerley, C.M., Monte, E., et al.
476 (2011) *Trichoderma*: The genomics of opportunistic success. *Nat Rev Microbiol*.

477 Du, F.Y., Ju, G.L., Xiao, L., Zhou, Y.M., and Wu, X. (2020) Sesquiterpenes and Cyclodepsipeptides from
478 Marine-Derived Fungus *Trichoderma longibrachiatum* and Their Antagonistic Activities against
479 Soil-Borne Pathogens. *Marine Drugs 2020, Vol 18, Page 165* **18**: 165.

480 El-Hasan, A., Walker, F., and Buchenauer, H. (2008) *Trichoderma harzianum* and its metabolite 6-
481 pentyl-alpha-pyrone suppress fusaric acid produced by *Fusarium moniliforme*. *Journal of*
482 *Phytopathology* **156**: 79–87.

483 Estrada-Rivera, M., Rebolledo-Prudencio, O.G., Pérez-Robles, D.A., Rocha-Medina, M.D.C., González-
484 López, M.D.C., and Casas-Flores, S. (2019) *Trichoderma* histone deacetylase HDA-2 modulates
485 multiple responses in *Arabidopsis*. *Plant Physiol* **179**: 1343–1361.

486 Evans, J.A., Eyre, C.A., Rogers, H.J., Boddy, L., and Müller, C.T. (2008) Changes in volatile production
487 during interspecific interactions between four wood rotting fungi growing in artificial media.
488 *Fungal Ecol*.

489 Feng, Y., Shuai, X., Chen, J., Zhang, Q., Jia, L., Sun, L., et al. (2025) Unveiling the Genomic Features
490 and Biocontrol Potential of *Trichoderma hamatum* Against Root Rot Pathogens. *Journal of*
491 *Fungi* **11**: 126.

492 Fernando, W.G.D., Ramarathnam, R., Krishnamoorthy, A.S., and Savchuk, S.C. (2005) Identification
493 and use of potential bacterial organic antifungal volatiles in biocontrol. *Soil Biol Biochem* **37**:
494 955–964.

495 Flores, C., Nieto, M., Millán-Gómez, D. V., Caro, M., Galindo, E., and Serrano-Carreón, L. (2019)
496 Elicitation and biotransformation of 6-pentyl-α-pyrone in *Trichoderma atroviride* cultures.
497 *Process Biochemistry* **82**: 68–74.

498 Garbeva, P. and Weisskopf, L. (2020) Airborne medicine: bacterial volatiles and their influence on
499 plant health. *New Phytologist* **226**: 32–43.

500 Garnica-Vergara, A., Barrera-Ortiz, S., Muñoz-Parra, E., Raya-González, J., Méndez-Bravo, A., Macías-
501 Rodríguez, L., et al. (2016) The volatile 6-pentyl-2H-pyran-2-one from *Trichoderma atroviride*
502 regulates *Arabidopsis* thaliana root morphogenesis via auxin signaling and ETHYLENE
503 INSENSITIVE 2 functioning. *New Phytologist*.

504 Ghorbanpour, M., Omidvari, M., Abbaszadeh-Dahaji, P., Omidvar, R., and Kariman, K. (2018)
505 Mechanisms underlying the protective effects of beneficial fungi against plant diseases.
506 *Biological Control* **117**: 147–157.

507 González-Pérez, E., Ortega-Amaro, M.A., Salazar-Badillo, F.B., Bautista, E., Douterlungne, D., and
508 Jiménez-Bremont, J.F. (2018) The *Arabidopsis-Trichoderma* interaction reveals that the fungal
509 growth medium is an important factor in plant growth induction. *Scientific Reports 2018 8:1* **8**:
510 1–14.

511 Guo, Y., Ghirardo, A., Weber, B., Schnitzler, J.P., Philipp Benz, J., and Rosenkranz, M. (2019a)
512 Trichoderma species differ in their volatile profiles and in antagonism toward ectomycorrhiza
513 Laccaria bicolor. *Front Microbiol* **10**:.

514 Hu, Z., Tao, Y., Tao, X., Su, Q., Cai, J., Qin, C., et al. (2019) Sesquiterpenes with Phytopathogenic Fungi
515 Inhibitory Activities from Fungus *Trichoderma virens* from *Litchi chinensis* Sonn. *J Agric Food*
516 *Chem* **67**: 10646–10652.

517 Hynes, J., Müller, C.T., Jones, T.H., and Boddy, L. (2007a) Changes in volatile production during the
518 course of fungal mycelial interactions between *Hypholoma fasciculare* and *Resinicium bicolor. J*
519 *Chem Ecol*.

520 Jeleń, H., Błaszczyk, L., Chełkowski, J., Rogowicz, K., and Strakowska, J. (2014a) Formation of 6-n-
521 pentyl-2H-pyran-2-one (6-PAP) and other volatiles by different Trichoderma species. *Mycol*
522 *Prog*.

523 Jin, X., Guo, L., Jin, B., Zhu, S., Mei, X., Wu, J., et al. (2020) Inhibitory mechanism of 6-Pentyl-2H-
524 pyran-2-one secreted by *Trichoderma atroviride* T2 against *Cylindrocarpon destructans*. *Pestic*
525 *Biochem Physiol*.

526 Kai, M., Effmert, U., and Piechulla, B. (2016) Bacterial-plant-interactions: Approaches to unravel the
527 biological function of bacterial volatiles in the rhizosphere. *Front Microbiol* **7**:.

528 Knowles, S.L., Raja, H.A., Roberts, C.D., and Oberlies, N.H. (2022) Fungal-fungal co-culture: a primer
529 for generating chemical diversity. *Nat Prod Rep* **39**:.

530 Lee, S., Behringer, G., Hung, R., and Bennett, J. (2019) Effects of fungal volatile organic compounds
531 on *Arabidopsis thaliana* growth and gene expression. *Fungal Ecol* **37**: 1–9.

532 Lee, S., Hung, R., Yap, M., and Bennett, J.W. (2015) Age matters: the effects of volatile organic
533 compounds emitted by *Trichoderma atroviride* on plant growth. *Arch Microbiol* **197**: 723–727.

534 Lee, S., Yap, M., Behringer, G., Hung, R., and Bennett, J.W. (2016) Volatile organic compounds
535 emitted by *Trichoderma* species mediate plant growth. *Fungal Biol Biotechnol* **3**: 7.

536 Li, N., Alfiky, A., Wang, W., Islam, M., Nourollahi, K., Liu, X., and Kang, S. (2018) Volatile Compound-
537 Mediated Recognition and Inhibition Between *Trichoderma* Biocontrol Agents and Fusarium
538 oxysporum. *Front Microbiol* **9**:.

539 Liu, X.H., Hou, X.L., Song, Y.P., Wang, B.G., and Ji, N.Y. (2020) Cyclonerane sesquiterpenes and an
540 isocoumarin derivative from the marine-alga-endophytic fungus *Trichoderma citrinoviride* A-
541 WH-20-3. *Fitoterapia* **141**: 104469.

542 Ma, H.X., Feng, X.J., Chen, Y., Chen, C.J., and Zhou, M.G. (2009) Occurrence and characterization of
543 dimethachlon insensitivity in *Sclerotinia sclerotiorum* in Jiangsu Province of China. *Plant Dis* **93**:
544 36–42.

545 Ma, X.Y., Song, Y.P., Shi, Z.Z., and Ji, N.Y. (2021) Three sesquiterpenes from the marine-alga-epiphytic
546 fungus *Trichoderma hamatum* Z36-7. *Phytochem Lett* **43**: 98–102.

547 Meena, M., Swapnil, P., Zehra, A., Dubey, M.K., and Upadhyay, R.S. (2017) Antagonistic assessment
548 of *Trichoderma* spp. by producing volatile and non-volatile compounds against different fungal
549 pathogens. *Archives of Phytopathology and Plant Protection* **50**: 629–648.

550 Mendoza-Mendoza, A., Esquivel-Naranjo, E.U., Soth, S., Whelan, H., Alizadeh, H., Echaide-Aquino,
551 J.F., et al. (2024) Uncovering the multifaceted properties of 6-pentyl-alpha-pyrone for control
552 of plant pathogens. *Front Plant Sci* **15**:.

553 Nemčovič, M., Jakubíková, L., Víden, I., and Farkaš, V. (2008) Induction of conidiation by endogenous
554 volatile compounds in *Trichoderma* spp. *FEMS Microbiol Lett* **284**: 231–236.

555 Nofiani, R., de Mattos-Shipley, K., Lebe, K.E., Han, L.C., Iqbal, Z., Bailey, A.M., et al. (2018) Strobilurin
556 biosynthesis in Basidiomycete fungi. *Nat Commun* **9**:.

557 O'Leary, J., Hiscox, J., Eastwood, D.C., Savoury, M., Langley, A., McDowell, S.W., et al. (2019) The
558 whiff of decay: Linking volatile production and extracellular enzymes to outcomes of fungal
559 interactions at different temperatures. *Fungal Ecol*.

560 Pennerman, K.K., Yin, G., and Bennett, J.W. (2022) Eight-carbon volatiles: prominent fungal and plant
561 interaction compounds. *J Exp Bot* **73**: 487–497.

562 Pezet, R., Pont, V., and Tabacchi, R. (1999) Simple analysis of 6-pentyl-α-pyrone, a major antifungal
563 metabolite of *Trichoderma* spp., useful for testing the antagonistic activity of these fungi.
564 *Phytochemical Analysis* **10**:.

565 Polizzi, V., Adams, A., Picco, A.M., Adriaens, E., Lenoir, J., Van Peteghem, C., et al. (2011) Influence of
566 environmental conditions on production of volatiles by *Trichoderma atroviride* in relation with
567 the sick building syndrome. *Build Environ*.

568 Rajani, P., Rajasekaran, C., Vasanthakumari, M.M., Olsson, S.B., Ravikanth, G., and Uma Shaanker, R.
569 (2021) Inhibition of plant pathogenic fungi by endophytic *Trichoderma* spp. through
570 mycoparasitism and volatile organic compounds. *Microbiol Res*.

571 Rao, Y., Zeng, L., Jiang, H., Mei, L., and Wang, Y. (2022) *Trichoderma atroviride* LZ42 releases volatile
572 organic compounds promoting plant growth and suppressing Fusarium wilt disease in tomato
573 seedlings. *BMC Microbiology 2022 22:1* **22**: 1–12.

574 Reithner, B., Brunner, K., Schuhmacher, R., Peissl, I., Seidl, V., Krska, R., and Zeilinger, S. (2005) The G
575 protein α subunit Tga1 of *Trichoderma atroviride* is involved in chitinase formation and
576 differential production of antifungal metabolites. *Fungal Genetics and Biology* **42**: 749–760.

577 Reithner, B., Schuhmacher, R., Stoppacher, N., Pucher, M., Brunner, K., and Zeilinger, S. (2007)
578 Signaling via the *Trichoderma atroviride* mitogen-activated protein kinase Tmk1 differentially
579 affects mycoparasitism and plant protection. *Fungal Genetics and Biology*.

580 Ryder, L.S., Harris, B.D., Soanes, D.M., Kershaw, M.J., Talbot, N.J., and Thornton, C.R. (2012)
581 Saprotrophic competitiveness and biocontrol fitness of a genetically modified strain of the
582 plant-growth-promoting fungus *Trichoderma hamatum* GD12. *Microbiology*.

583 Ryu, C.M., Farag, M.A., Hu, C.H., Reddy, M.S., Kloepper, J.W., and Paré, P.W. (2004) Bacterial
584 volatiles induce systemic resistance in *Arabidopsis*. *Plant Physiol*.

585 Ryu, C.M., Faragt, M.A., Hu, C.H., Reddy, M.S., Wei, H.X., Paré, P.W., and Kloepper, J.W. (2003)
586 Bacterial volatiles promote growth in *Arabidopsis*. *Proc Natl Acad Sci U S A*.

587 Scarselletti, R. and Faull, J.L. (1994) In vitro activity of 6-pentyl-α-pyrone, a metabolite of
588 *Trichoderma harzianum*, in the inhibition of *Rhizoctonia solani* and *Fusarium oxysporum* f. sp.
589 lycopersici. *Mycol Res* **98**: 1207–1209.

590 Scherlach, K. and Hertweck, C. (2021) Mining and unearthing hidden biosynthetic potential. *Nat*
591 *Commun*.

592 Schroeckh, V., Scherlach, K., Nützmann, H.W., Shelest, E., Schmidt-Heck, W., Schuemann, J., et al.
593 (2009) Intimate bacterial-fungal interaction triggers biosynthesis of archetypal polyketides in
594 *Aspergillus nidulans*. *Proc Natl Acad Sci U S A* **106**: 14558–14563.

595 Schulz-Bohm, K., Martín-Sánchez, L., and Garbeva, P. (2017) Microbial Volatiles: Small Molecules
596 with an Important Role in Intra- and Inter-Kingdom Interactions. *Front Microbiol* **8**: 1–10.

597 Serrano-Carreón, L., Flores, C., Rodríguez, B., and Galindo, E. (2004) *Rhizoctonia solani*, an elicitor of
598 6-pentyl-α-pyrone production by *Trichoderma harzianum* in a two liquid phases, extractive
599 fermentation system. *Biotechnol Lett*.

600 Shaw, S., Le Cocq, K., Paszkiewicz, K., Moore, K., Winsbury, R., De Torres Zabala, M., et al. (2016)
601 Transcriptional reprogramming underpins enhanced plant growth promotion by the biocontrol
602 fungus *Trichoderma hamatum* GD12 during antagonistic interactions with *Sclerotinia*
603 *sclerotiorum* in soil. *Mol Plant Pathol*.

604 Shi, X.-S., Song, Y.-P., Meng, L.-H., Yang, S.-Q., Wang, D.-J., Zhou, X.-W., et al. (2021) Isolation and
605 Characterization of Antibacterial Carotane Sesquiterpenes from *Artemisia argyi* Associated
606 Endophytic *Trichoderma virens* QA-8. *Antibiotics 2021, Vol 10, Page 213* **10**: 213.

607 Shi, Z.Z., Fang, S.T., Miao, F.P., Yin, X.L., and Ji, N.Y. (2018) Trichocarotins A–H and trichocadinin A,
608 nine sesquiterpenes from the marine-alga-epiphytic fungus *Trichoderma virens*. *Bioorg Chem*
609 **81**: 319–325.

610 Shi, Z.Z., Liu, X.H., Li, X.N., and Ji, N.Y. (2020) Antifungal and Antimicroalgal Trichothecene
611 Sesquiterpenes from the Marine Algicolous Fungus *Trichoderma brevicompactum* A-DL-9-2. *J*
612 *Agric Food Chem* **68**: 15440–15448.

613 Silva, L.R. da, Valadares-Inglis, M.C., Peixoto, G.H.S., Luccas, B.E.G. de, Muniz, P.H.P.C., Magalhães,
614 D.M., et al. (2021) Volatile organic compounds emitted by *Trichoderma azevedoi* promote the
615 growth of lettuce plants and delay the symptoms of white mould. *Biological Control* **152**:
616 104447.

617 Speckbacher, V., Ruzsanyi, V., Wigger, M., and Zeilinger, S. (2020) The *Trichoderma atroviride* Strains
618 P1 and IMI 206040 Differ in Their Light-Response and VOC Production. *Molecules 2020, Vol 25,*
619 *Page 208* **25**: 208.

620 Speckbacher, V., Zeilinger, S., Zimmermann, S., Mayhew, C.A., Wiesenhofer, H., and Ruzsanyi, V.
621 (2021) Monitoring the volatile language of fungi using gas chromatography-ion mobility
622 spectrometry. *Anal Bioanal Chem*.

623 Stoppacher, N., Kluger, B., Zeilinger, S., Krska, R., and Schuhmacher, R. (2010) Identification and
624 profiling of volatile metabolites of the biocontrol fungus *Trichoderma atroviride* by HS-SPME-
625 GC-MS. *J Microbiol Methods*.

626 Studholme, D.J., Harris, B., Le Cocq, K., Winsbury, R., Perera, V., Ryder, L., et al. (2013) Investigating
627 the beneficial traits of *Trichoderma hamatum* GD12 for sustainable agriculture—insights from
628 genomics. *Front Plant Sci*.

629 Thomas, G., Rusman, Q., Morrison, W.R., Magalhães, D.M., Dowell, J.A., Ngumbi, E., et al. (2023)
630 Deciphering Plant-Insect-Microorganism Signals for Sustainable Crop Production. *Biomolecules*
631 **13**: 997.

632 Thomas, G., Withall, D., and Birkett, M. (2020) Harnessing microbial volatiles to replace pesticides
633 and fertilizers. *Microb Biotechnol* **13**: 1366–1376.

634 Tribe, H.T. (1957) On the parasitism of *Sclerotinia trifoliorum* by *Coniothyrium minitans*. *Transactions*
635 *of the British Mycological Society* **40**: 489–499.

636 Tyc, O., de Jager, V.C.L., van den Berg, M., Gerards, S., Janssens, T.K.S., Zaagman, N., et al. (2017)
637 Exploring bacterial interspecific interactions for discovery of novel antimicrobial compounds.
638 *Microb Biotechnol* **10**: 910–925.

639 Tyc, O., Zweers, H., de Boer, W., and Garbeva, P. (2015) Volatiles in inter-specific bacterial
640 interactions. *Front Microbiol* **6**:.

641 Vinale, F., Nicoletti, R., Borrelli, F., Mangoni, A., Parisi, O.A., Marra, R., et al. (2017) Co-Culture of
642 Plant Beneficial Microbes as Source of Bioactive Metabolites. *Sci Rep*.

643 Wang, Y., Li, X.M., Yang, S.Q., Zhang, F.Z., Wang, B.G., Li, H.L., and Meng, L.H. (2022) Sesquiterpene
644 and Sorbicillinoid Glycosides from the Endophytic Fungus *Trichoderma longibrachiatum* EN-586
645 Derived from the Marine Red Alga *Laurencia obtusa*. *Marine Drugs 2022, Vol 20, Page 177* **20**:
646 177.

647 Weisskopf, L., Schulz, S., and Garbeva, P. (2021) Microbial volatile organic compounds in intra-
648 kingdom and inter-kingdom interactions. *Nat Rev Microbiol* **19**: 391–404.

649 Westhoff, S., van Wezel, G.P., and Rozen, D.E. (2017) Distance-dependent danger responses in
650 bacteria. *Curr Opin Microbiol*.

651 Wonglom, P., Ito, S. ichi, and Sunpapao, A. (2020) Volatile organic compounds emitted from
652 endophytic fungus *Trichoderma asperellum* T1 mediate antifungal activity, defense response
653 and promote plant growth in lettuce (*Lactuca sativa*). *Fungal Ecol* **43**:.

654 Woo, S.L., Hermosa, R., Lorito, M., and Monte, E. (2023) *Trichoderma*: a multipurpose, plant-
655 beneficial microorganism for eco-sustainable agriculture. *Nat Rev Microbiol* **21**:.

656 Xie, S., Liu, J., Gu, S., Chen, X., Jiang, H., and Ding, T. (2020) Antifungal activity of volatile compounds
657 produced by endophytic *Bacillus subtilis* DZSY21 against Curvularia lunata. *Ann Microbiol*.

658 Xiong, C., Li, Q., Li, S., Chen, C., Chen, Z., and Huang, W. (2017) *In vitro* antimicrobial activities and
659 mechanism of 1-octen-3-ol against food-related bacteria and pathogenic fungi. *J Oleo Sci* **66**:
660 1041–1049.

661 Yin, G., Zhang, Y., Fu, M., Hua, S.S.T., Huang, Q., Pennerman, K.K., et al. (2019) Influence of R and S
662 enantiomers of 1-octen-3-ol on gene expression of *Penicillium chrysogenum*. *J Ind Microbiol*
663 *Biotechnol* **46**: 977–991.

664 Zhang, D., Yu, S., Yang, Y., Zhang, J., Zhao, D., Pan, Y., et al. (2020) Antifungal Effects of Volatiles
665 Produced by *Bacillus subtilis* Against *Alternaria solani* in Potato. *Front Microbiol*.

666 Zhang, F., Yang, X., Ran, W., and Shen, Q. (2014*) Fusarium oxysporum* induces the production of
667 proteins and volatile organic compounds by *Trichoderma harzianum* T-E5. *FEMS Microbiol Lett*
668 **359**: 116–123.

669 Zou, C., Li, Z., and Yu, D. (2010) *Bacillus megaterium* strain XTBG34 promotes plant growth by
670 producing 2-pentylfuran. *Journal of Microbiology* **48**: 460–466.

671

672

673 **Figure legends.**

674 Figure 1 | Dual-culture confrontation assays of (a) self-challenged *Trichoderma hamatum* GD12 strain;
675 (b) self-challenged *Sclerotinia sclerotiorum* (c) co-culture of *S. sclerotiorum* (top) and *T. hamatum*
676 GD12 (bottom); (d) self-challenged *T. hamatum* N-acetyl-β-glucosaminidase (*ΔThnag::hph*) mutant;
677 (e) self-challenged *S. sclerotiorum*; (f) co-culture of *S sclerotiorum* (top) and *T. hamatum ΔThnag::hph*
678 mutant (bottom).

679 Figure 2 | Representative gas chromatographic analysis of volatile organic compounds (VOCs)
680 collected by air entrainment from 7-day old cultures of (a) uninoculated growth media (control), (b)
681 self-challenged *S. sclerotiorum*, (c) self-challenged *T. hamatum* GD12, and (d) *T. hamatum* GD12 co-
682 inoculated with *S. sclerotiorum*. For an explanation of peak numbers, see Table 1.

683 Figure 3 | Production of VOCs in treatments of *Trichoderma hamatum GD12* and *S. sclerotiorurm* co-
684 culture treatments over the course of 24 days for three VOCs. Bars represent the peak area value of
685 each VOC (± SD) (n=3).

686 Figure 4 | Representative gas chromatographic (on an HP-1 column) analysis of VOCs from dynamic
687 headspace collections of 7-day old cultures of (a) uninoculated growth media (control), (b) self-
688 challenged *S. sclerotiorum*, (c) self-challenged *T. hamatum ΔThnag::hph*, and (d) *T. hamatum*
689 *ΔThnag::hph* co-inoculated with *S. sclerotiorum*.

690 Figure 5 | Antifungal activities of selected VOCs on the growth of *S. sclerotiorum*. *S. sclerotiorum* was
691 incubated with selected VOCs at 45.5 µM doses and the inhibition rates were calculated relative to
692 control plates (exposed to diethyl ether alone) after 3 days. Bars represent the mean mycelial area of
693 *S. sclerotiorum* upon exposure to each VOC (± SD) (n=3). Different letters indicate significant
694 differences between treatments according to Tukey's multiple comparisons test ($p < 0.05$). Y axis
695 represents mycelial area (mm^2).

696 Figure 6 | Antifungal activities of selected VOCs on the growth of *S. sclerotiorum*, at reduced doses.
697 Bars represent the mean mycelial area of *S. sclerotiorum* upon exposure to each VOC (± SD) (n=3).
698 Different letters indicate significant differences between treatments according to Tukey's multiple
699 comparisons test ($p < 0.05$). Y axis represents mycelial area (mm^2).

700 Figure 7 | Antifungal activities of selected VOCs on the growth of *S. sclerotiorum*, representing
701 individual structural components of 1-octen-3-one, at 45.5 µM. Bars represent the mycelial area of *S.*
702 *sclerotiorum* upon exposure to each VOC (± SD) (n=3). Different letters indicate significant differences
703 between treatments according to Tukey's multiple comparisons test ($p < 0.05$).

704 Figure 8 | Antifungal activities of 6-PAP and 1-octen-3-one, on *Sclerotinia sclerotiorum* at 45.5 µM.

705

706

707

708

709

710

711

712

713

714

715

716

717

718

719

720

721

722

723

724

725

726

727 Figure 1.

728

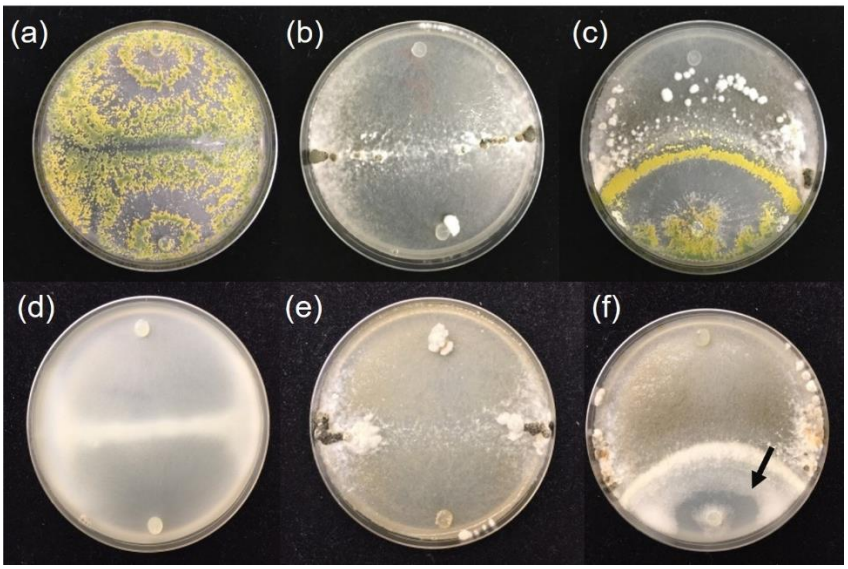
(a)
(b)
(c)
(d)
(e)
(f)

747 Figure 2.

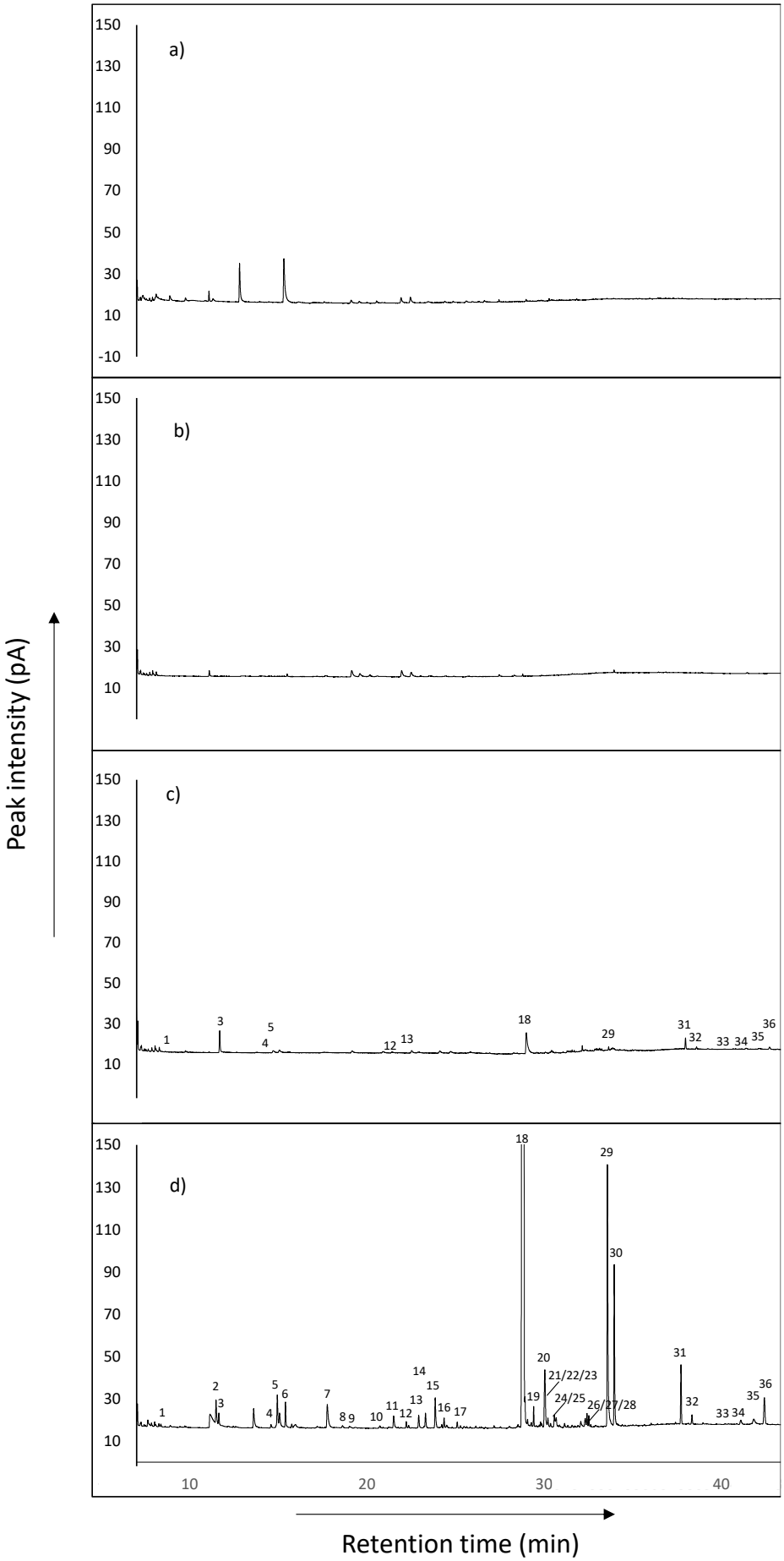
a)
b)
c)
d)
Peak intensity (pA)
Retention time (min)
150
130
110
90
70
50
30
10
-10
10
20
30
40
1
2
3
4
5
6
7
8
9
10
11
12
13
14
15
16
17
18
19
20
21/22/23
24/25
26/27/28
29
30
31
32
33
34
35
36

748

749 **Figure 3.**

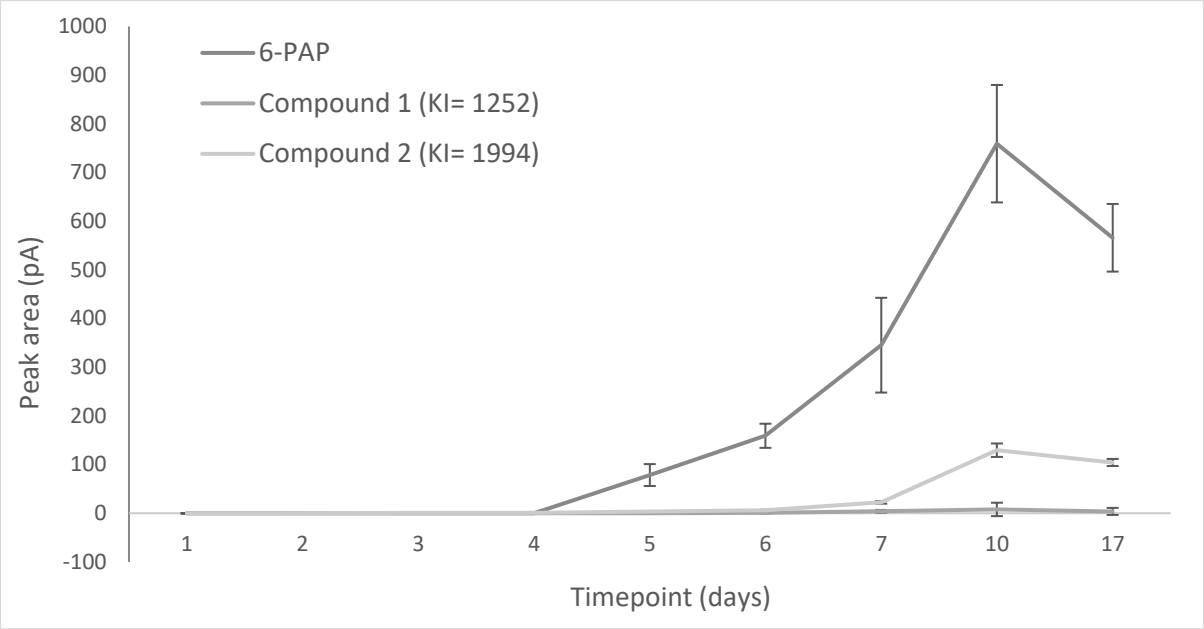

750

751

752

753

754

755

756

757

758

759

760

761

762

763

764

765

Figure 4.

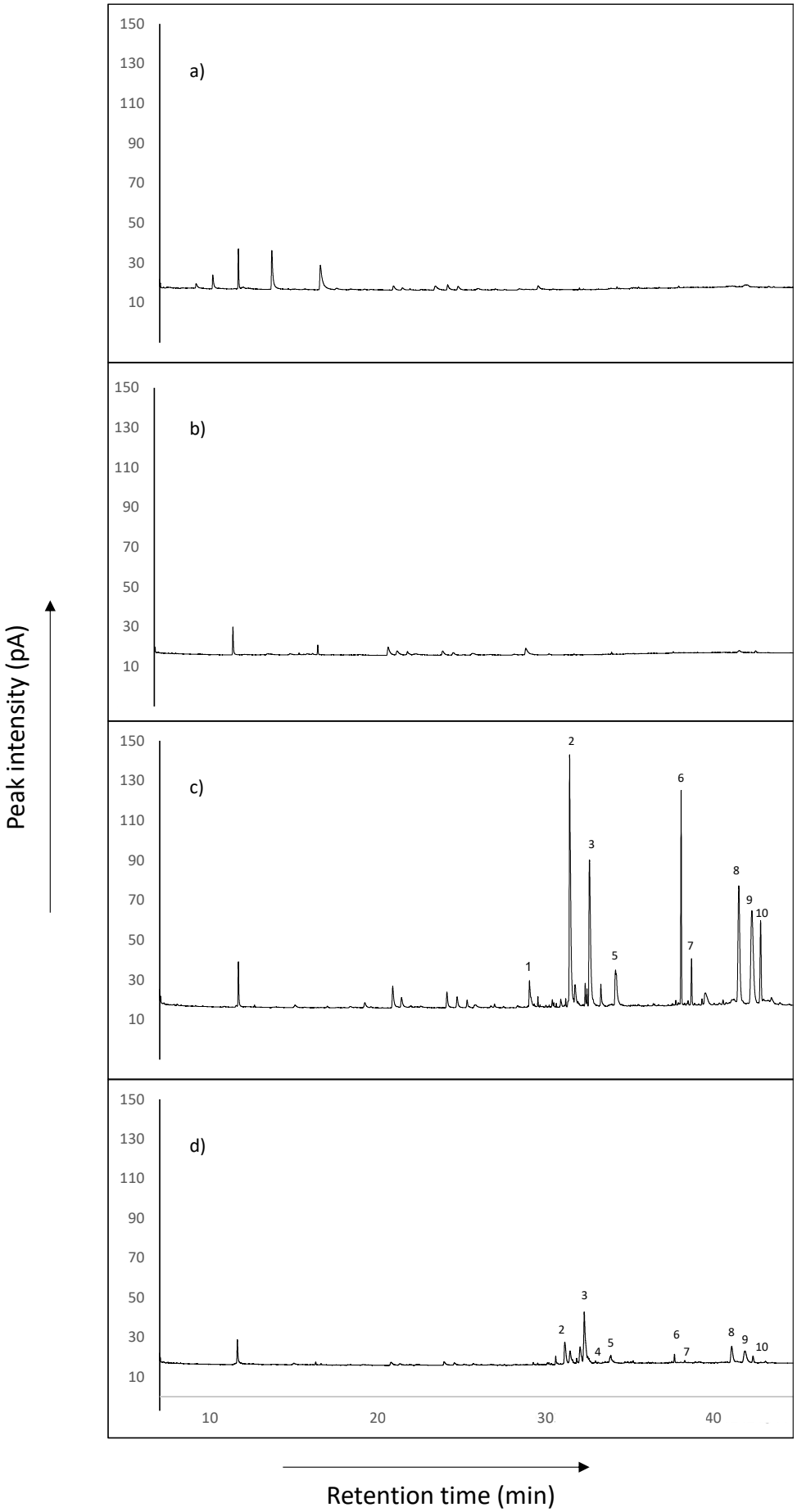
a)
b)
c)
d)
Peak intensity (pA)
Retention time (min)
150
130
110
90
70
50
30
10
10
20
30
40
1
2
3
4
5
6
7
8
9
10

768

Figure 5.

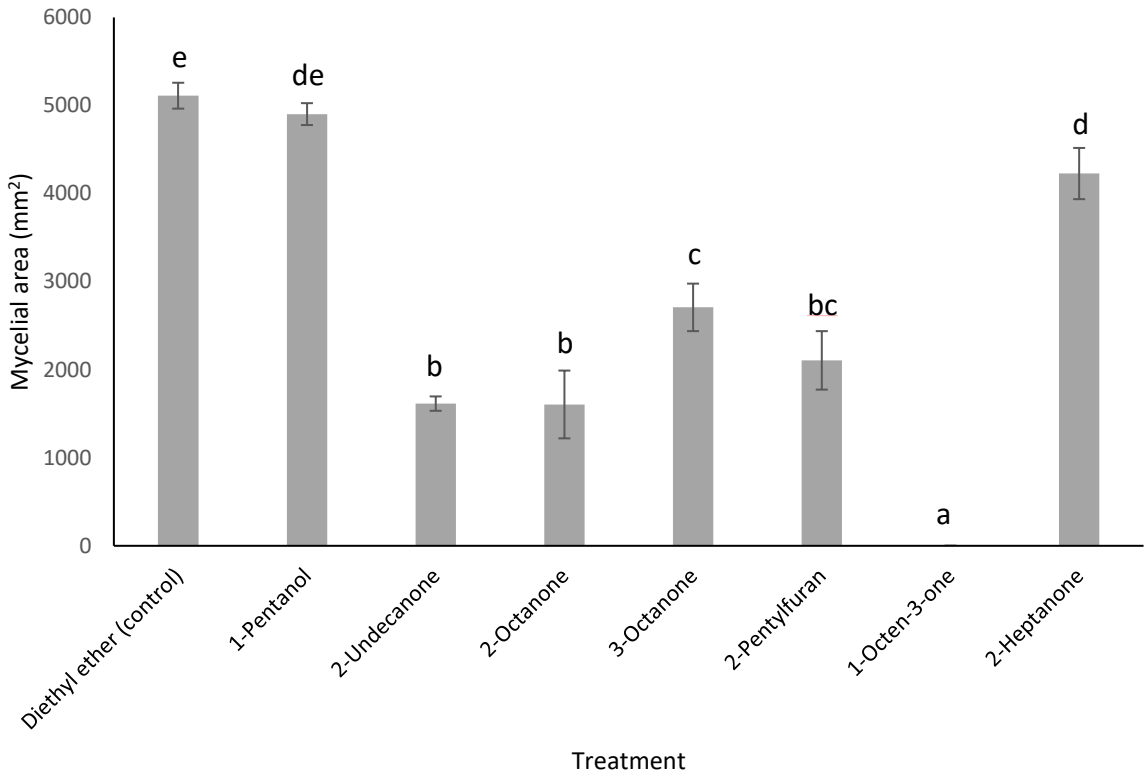
6000
5000
4000
3000
2000
1000
0
Mycelial area (mm²)
e
de
b
b
c
bc
a
d
Diethyl ether (control)
1-Pentanol
2-Undecanone
2-Octanone
3-Octanone
2-Pentylfuran
1-Octen-3-one
2-Heptanone
Treatment

Figure 6.

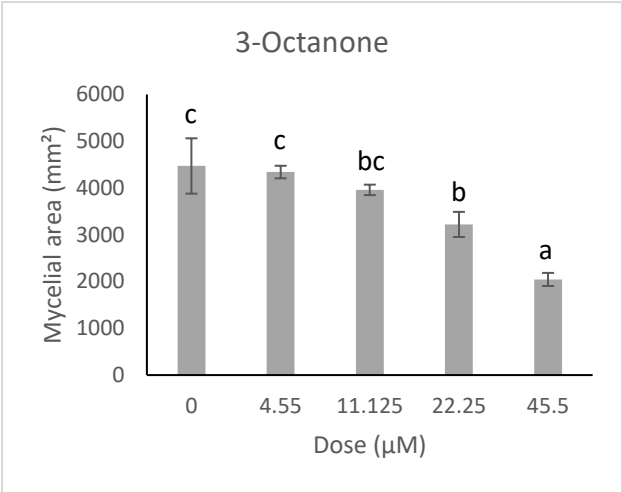
3-Octanone
Mycelial area (mm²)
6000
5000
4000
3000
2000
1000
0
c
c
bc
b
a
0
4.55
11.125
22.25
45.5
Dose (µM)

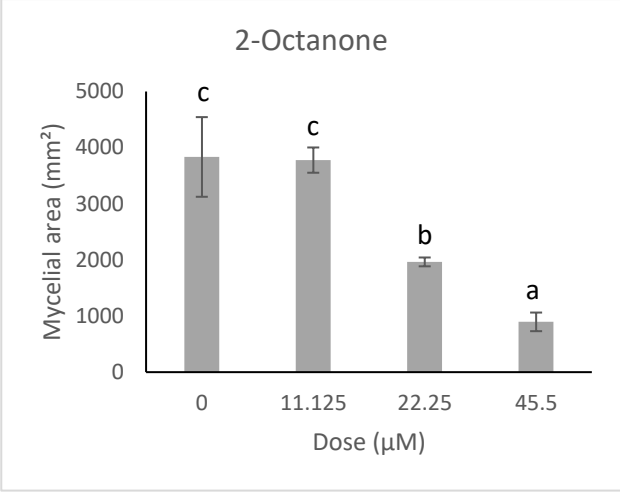
2-Octanone
Mycelial area (mm²)
5000
4000
3000
2000
1000
0
c
c
b
a
0
11.125
22.25
45.5
Dose (µM)

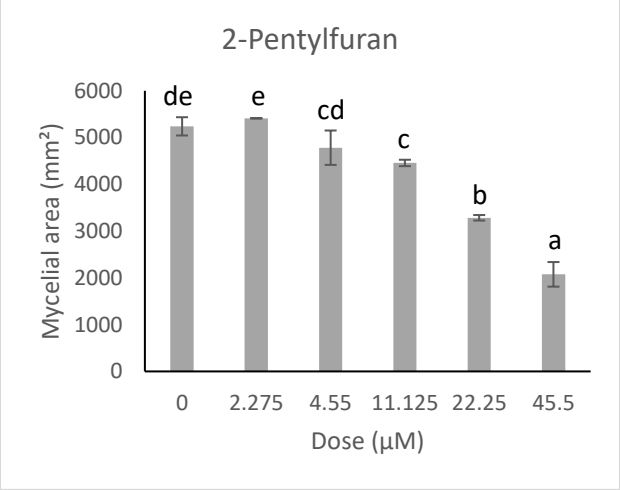
2-Pentylfuran
Mycelial area (mm²)
6000
5000
4000
3000
2000
1000
0
de
e
cd
c
b
a
0
2.275
4.55
11.125
22.25
45.5
Dose (µM)

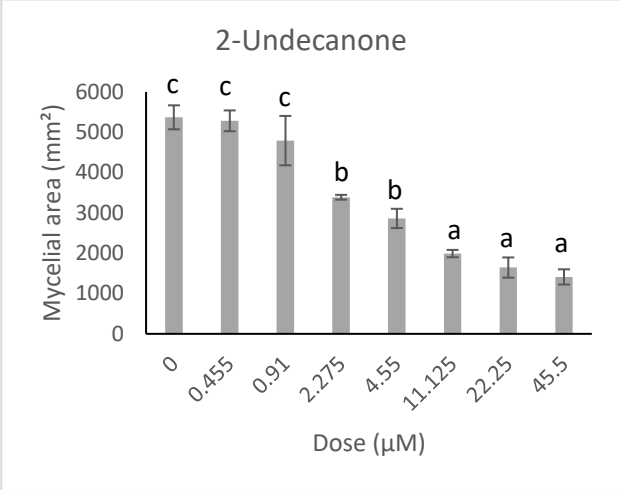
2-Undecanone
Mycelial area (mm²)
6000
5000
4000
3000
2000
1000
0
c
c
c
b
b
a
a
a
0
0.455
0.91
2.275
4.55
11.125
22.25
45.5
Dose (µM)

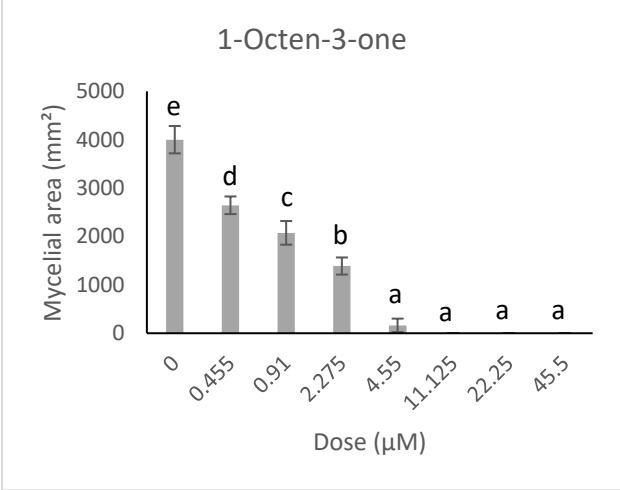
1-Octen-3-one
Mycelial area (mm²)
5000
4000
3000
2000
1000
0
e
d
c
b
a
a
a
a
0
0.455
0.91
2.275
4.55
11.125
22.25
45.5
Dose (µM)

814

815

816

817 Figure 7.

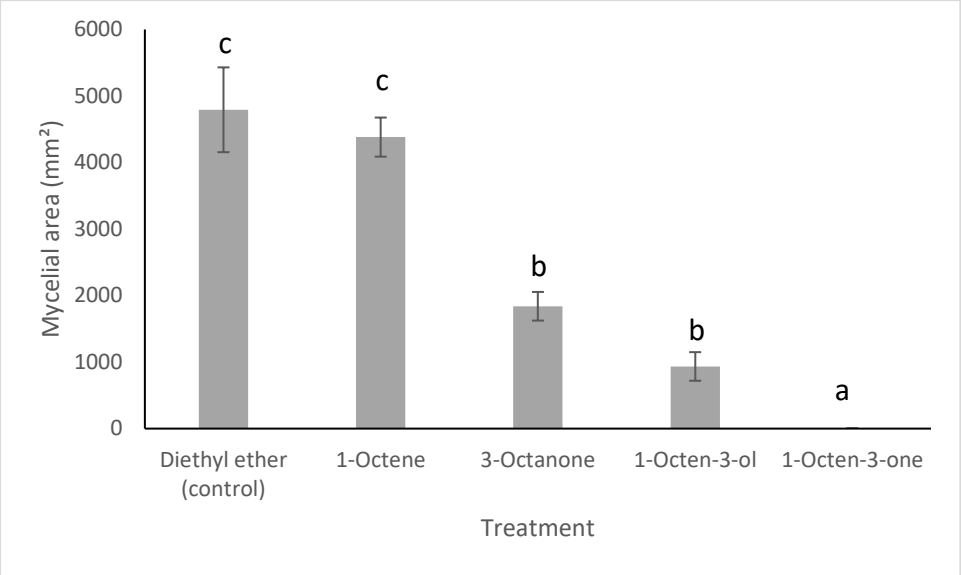

818

819

820

821

822

823

824

825

826 Figure 8.

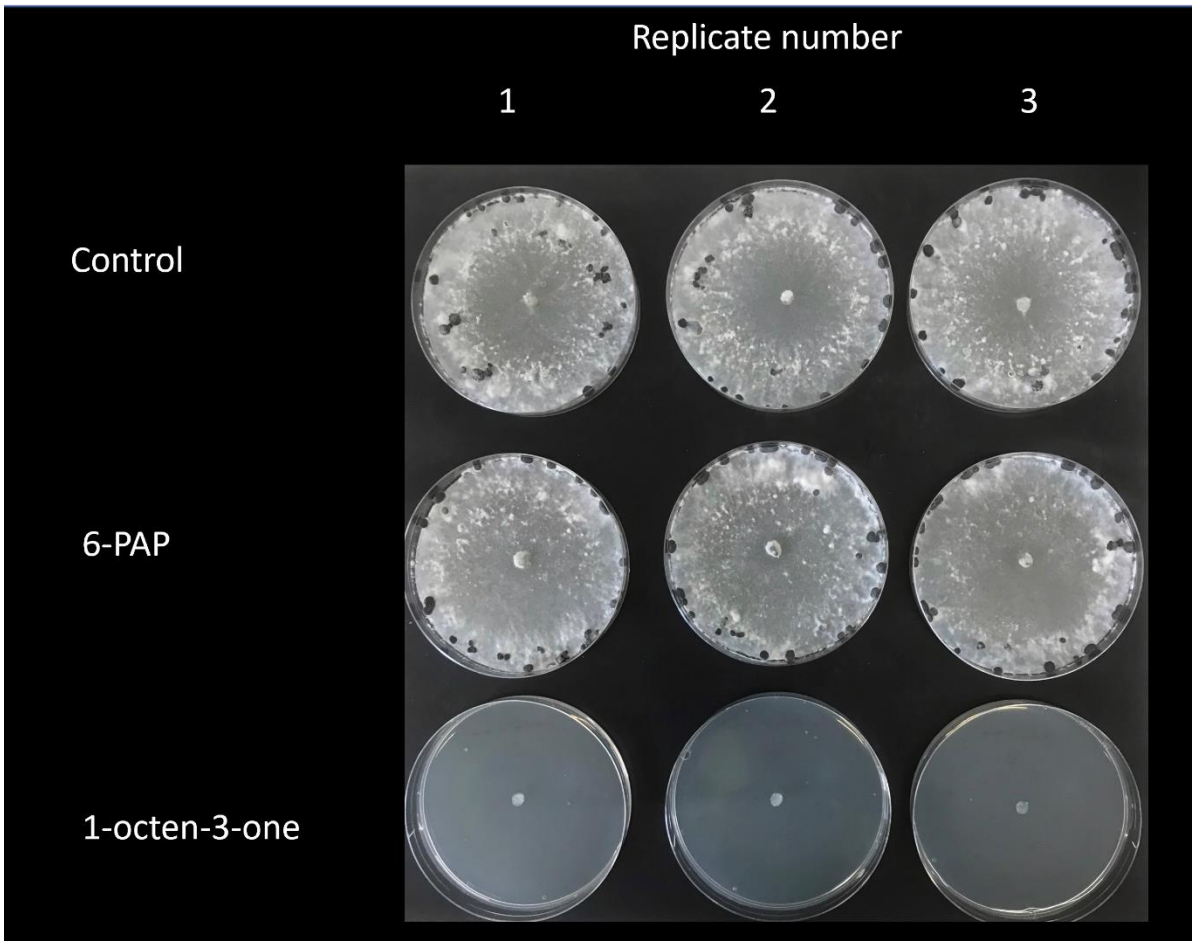

827

828

829

830

831

Table 1 | Composition of VOCs from dynamic headspace collections of 7-day old cultures of self-challenged *T. hamatum* GD12, or GD12 co-inoculated with *S. sclerotiorum* (n=4) (mean peak area ± SE). Data were analysed by Student's t-test ($p < 0.05$). KIs on a non-polar HP-1 GC column.

Peak no.	Compound	KI	GD12 vs S. sclerotiorum	GD12 vs GD12	p value
1	1-Pentanol*	**754**	**7.29 (± 1.85)**	2.42(±0.37)	0.016
2	2(5H)-Furanone	**871**	**95.43 (± 24.50)**	n.d.	NA
3	2-Heptanone*	**876**	26.08(±4.82)	26.47(±7.6)	0.813
4	1-Octen-3-one*	**959**	8.76(±3.92)	11.49(±9.23)	0.606
5	3-Octanone*	**969**	50.98(±17.87)	41.25(±22.83)	0.439
6	2-Octanone*	**972**	**29.00(±6.52)**	n.d.	NA
7	2-Pentylfuran*	**981**	**142.00(± 48.95)**	n.d.	NA
8	No i.d.	**990**	**4.65(±0.44)**	n.d.	NA
9	No i.d.	**995**	**6.90(±1.81)**	n.d.	NA
10	No i.d.	**1049**	**30.67(±13.89)**	n.d.	NA
11	No i.d.	**1074**	**8.98(±1.59)**	n.d.	NA
12	No i.d.	**1137**	25.29(±12.24)	20.34(±13.59)	0.621
13	2-n-Heptylfuran	**1182**	12.60(±3.31)	7.61(±4.01)	0.278
14	Cyclodecanone	**1217**	**28.09(±9.8)**	n.d.	NA
15	2-Butyl-cyclodecanone	**1235**	**71.50(±29.64)**	n.d.	NA
16	No i.d.	**1252**	**53.66(±34.92)**	n.d.	NA
17	2-Undecanone*	**1276**	**9.00(±1.54)**	n.d.	NA
18	6-Pentyl-2H-pyran-2-one*	**1429**	**7596.41(±1617.76)**	58.04(±20.08)	0.001
19	No i.d.	**1457**	**27.35(±5.69)**	n.d.	NA
20	No i.d.	**1488**	**90.47(±24.10)**	n.d.	NA
21	No i.d.	**1497**	**14.21(±4.25)**	n.d.	NA
22	No i.d.	**1505**	**8.65(±1.61)**	n.d.	NA
23	No i.d.	**1518**	**8.12(±2.04)**	n.d.	NA
24	No i.d.	**1565**	**12.03(±5.38)**	n.d.	NA
25	No i.d.	**1608**	**6.67(±0.54)**	n.d.	NA
26	No i.d.	**1625**	**11.33(±2.90)**	n.d.	NA
27	No i.d.	**1632**	**14.44(±3.66)**	n.d.	NA
28	No i.d.	**1639**	**12.89(±3.51)**	n.d.	NA
29	No i.d.	**1710**	**334.61(±103.98)**	5.19(±3.42)	0.004
30	No i.d.	**1739**	**98.07(±42.20)**	n.d.	NA
31	No i.d.	**2018**	**68.41(±14.13)**	7.67(±2.77)	0.002
32	No i.d.	**2057**	**9.81(±2.14)**	1.45(±0.67)	0.003
33	No i.d.	**2198**	2.40(±0.77)	0.65(±0.39)	0.105
34	No i.d.	**2208**	**8.00(±1.56)**	1.60(±0.69)	0.006
35	No i.d.	**2240**	11.00(±3.56)	1.55(±0.78)	0.043
36	No i.d.	**2266**	**43.73(±8.74)**	2.85(±0.72)	0.001

n.d. not detected

858 Table 2 | Composition of VOCs collected from dynamic headspace collections of 7-day old cultures of
859 self-challenged *T. hamatum ΔThnag::hph*, or *ΔThnag::hph* co-inoculated with *S. sclerotiorum* (n=4)
860 (mean peak area ± SE). Data were analysed by Student's t-test ($p < 0.05$). KIs on a non-polar HP-1 GC
861 column.

			Mean (± SEM)		
Peak no.	**KI**	**Compound**	**nag vs *S. sclerotiorum***	**nag vs nag**	**p value**
1	1425	6-Pentyl-2H-pyran-2-one*	n.d.	52.06 (±17.40)	NA
2	1552	No i.d.	61.89(±21.1)	**793(±213.9)**	0.049
3	1624	No i.d.	189.32(±69.91)	526.03(±145.52)	0.278
4	1692	No i.d.	**1.9(±0.78)**	0	
5	1735	No i.d.	26.14(±9.06)	161.8(±53.61)	0.118
6	2016	No i.d.	51.09(±2.80)	**322.7(±66.90)**	0.001
7	2055	No i.d.	3.37(±1.20)	**80.3(±16.74)**	0.003
8	2208	No i.d.	74.87(±28.26)	336.83(±78.090	0.15
9	2243	No i.d.	76.49(±28.95)	367(±90.19)	0.145
10	2264	No i.d.	22.31(±2.91)	**271.00(±67.83)**	0.005

862

863